LA-UR-15-21099 (Accepted Manuscript)

Transmission Electron Microscope In Situ Straining Technique to Directly Observe Defects and Interfaces During Deformation in Magnesium

Morrow, Benjamin
Cerreta, Ellen Kathleen
Mccabe, Rodney James
Tome, Carlos

To be published in: JOM

DOI to publisher's version: 10.1007/s11837-015-1432-6

Permalink to record: http://permalink.lanl.gov/object/view?what=info:lanl-repo/lareport/LA-UR-15-21099

A TEM in-situ straining technique to directly observe defects and interfaces during deformation in magnesium

For JOM Issue on "*In-Situ Mechanical Testing in Electron Microscopes"*

B. M. Morrow, E. K. Cerreta, R. J. McCabe, C. N. Tomé

MST Division, Los Alamos National Laboratory; P.O. Box 1663, Los Alamos, NM, 87545 USA
Email address: morrow@lanl.gov (B.M. Morrow)

Paper type: Research Summary: 3–5 printed pages (2,400–4,000 words). Outlines recent, technically in-depth investigations in materials science and technology.

Abstract (150-250 words)
In-situ straining was used to study deformation behavior of hexagonal close-packed (hcp) metals. Twinning and dislocation motion, both essential to plasticity in hcp materials, were observed. Typically, these processes are characterized post-mortem by examining remnant microstructural features after straining has occurred. By imposing deformation during imaging, direct observation of active deformation mechanisms is possible. This work focuses on straining of structural metals in a transmission electron microscope (TEM), and a recently developed technique that utilizes familiar procedures and equipment to increase ease of experiments. In-situ straining in a TEM presents several advantages over conventional post-mortem characterization, most notably time-resolution of deformation and streamlined identification of active deformation mechanisms. Drawbacks to the technique and applicability to other studies are also addressed. In-situ straining is used to study twin boundary motion in hcp magnesium. A $\{10\bar{1}2\}$ twin was observed during tensile and compressive loading. Twin-dislocation interactions are directly observed. Notably, dislocations are observed to remain mobile, even after multiple interactions with twin boundaries, a result which suggests that Basinki's dislocation transformation mechanism by twinning is not present in hcp metals. The coupling of in-situ straining with traditional post-mortem characterization yields more detailed information about material behavior during deformation than either technique alone.

Keywords: transmission electron microscopy (TEM); in-situ mechanical testing; twinning; magnesium;

Introduction

In-situ straining techniques are receiving increasing attention in the study of mechanical behavior of materials. Many techniques have been used to probe in-situ material response to a stimulus across many length scales, including optical microscopy [1], scanning and transmission electron microscopy[2–4], and x-ray [5,6] and neutron diffraction [7,8]. Electron microscopy, in particular, is well suited to study materials at the nanoscale. While the practice of performing in-situ experiments in an electron microscope to probe material response during imaging has been around for decades, it represents a very small fraction of electron microscopy studies. More common are post-mortem techniques, which interrogate material microstructure before or after an experiment. Even so, in-situ experiments have made important contributions to the areas of solid-state phase transformations, irradiation damage, recovery and recrystallization, deformation and creep, electrochemical and environmental effects, and electronic and magnetic properties, and others [9–11]. Of specific importance to structural materials is the deformation behavior under applied loads. Initial work in this area utilized thermal stresses caused by heating due to the electron beam itself to drive microstructural features such as dislocations [12–14]. Subsequently, specialized transmission electron microscope (TEM) holders were developed that could drive deformation directly by straining a thin foil specimen [15–17]. This allowed for the direct observation of microstructure during plasticity. Motion of dislocations is of particular importance in ductile metals. Subsequently, this topic has been studied in-situ for a wide range of materials and loading conditions [18–27]. For hexagonal close-packed (hcp) metals like magnesium, titanium, zirconium, and their alloys, twinning is also extremely important for plasticity [28,29]. Unlike dislocation motion, which (per dislocation) affects a small volume of material, and often occurs on a relatively long timescale [30], twinning represents a massive, rapid reorientation of a crystal often encompassing a large volume fraction of the material [31–33]. Additionally, because of the crystallographic nature of twinning, during growth, twin boundaries must often propagate through a microstructure that already includes dislocation content or other microstructural features [34]. A detailed understanding of the active mechanisms involved in plasticity, their kinetics, and interactions between different mechanisms is critical to understanding the bulk plastic behavior during deformation in hcp metals. In-situ straining is uniquely capable of delivering this type of information, which would be difficult (or in some cases impossible) to measure using post-mortem techniques alone. A previous studies have used in-situ straining to observe twin-twin interactions, and characterize twin boundary structure in magnesium and zirconium [4,34]. The present study will also present in-situ straining results, but focus instead on twin interactions with dislocations.

Experimental Procedure

Specimen Preparation

A site-specific technique was used to prepare samples for in-situ mechanical testing. First, bulk material was deformed to create microstructural features of interest. Cuboidal samples were machined from a high-purity (99.96%) Mg hot-rolled plate which had been heat-treated at 473 K (200 °C) for 30 min, resulting in a twin-free, equiaxed grain structure. Detailed compositional analysis has been reported previously [3]. Samples were loaded in compression in an orientation conducive to deformation twinning to 1% strain to generate initial twin content, and sectioned for viewing in the compression direction. Samples were prepared using 1200 grit SiC paper,

followed by a solution of 10% nitric acid in water to remove surface damage and provide a suitable surface for electron backscatter diffraction (EBSD).

An FEI Company (FEI) Inspect scanning electron microscope (SEM) with an EDAX Orientation Imaging Microscopy (OIM) data collection system was used to collect EBSD scans. The EBSD data enabled triage of the bulk specimens to locate regions of interest for subsequent specimen preparation and mechanical testing. An FEI Helios dual beam focused ion beam (FIB) was used to prepare microtensile TEM samples from the bulk. Figure 1 shows the inverse pole figure (IPF) map for the specimen examined in this work. The black box in Figure 1a shows the approximate location where the site-specific tensile specimen was extracted using FIB. In this work, each in-situ TEM tensile specimen was cut from a single grain containing a $(10\bar{1}2)$ tensile twin, with the tensile axis of the specimen aligned parallel to the c-axis of the parent grain. This orientation was selected to promote twin growth during tensile testing. Another advantage of the site-specific approach is that it allows for the selection of a specific TEM viewing direction (in this case, approximately parallel to $[1\bar{2}10]$ corresponding to an on-edge view of the $(10\bar{1}2)$ twin boundary) to allow for convenient imaging in the TEM. This is especially important, as the TEM holder used to strain the samples has only a single tilt axis, reducing the available tilt space (and thus reducing the total accessible imaging conditions). The final viewing direction of the TEM foil is vertical relative to the sample surface in Figure 1a. The tensile direction is horizontal and the TEM foil extends several microns into the surface (plane of page). Figure 2 shows a schematic of the entire process of specimen preparation for site-specific, in-situ mechanical testing in TEM. This method is described in greater detail in the literature [35], but will be summarized here. The foil was cut and thinned using common FIB techniques, plucked from the sample, and fixed to a larger tensile dogbone (11.5 mm in length, 2.5 mm wide, and 150 microns thick, with a 1 mm length on one side thinned to a knife-edge). A small slot was prepared along the knife-edge using FIB, and the TEM foil was secured so that it bridged the open slot. The straining forces are applied to this larger dogbone, and these forces are transmitted to the thin foil. The electron transparent region of a typical tensile specimen prepared using this technique is 8-12 μm in the tension direction and 5-10 μm in width. A Gatan single-tilt, in-situ, straining TEM holder is used to impose loading forces on the prepared dogbones. An FEI Tecnai with an accelerating voltage of 300kV is used for imaging. Displacement rates are between 0.1 and 1 μm/s for tensile loads, and ~1 μm/s for compressive loading. Due to the rapid rate of microstructural change inherent to twinning processes, the specimen was strained intermittently to allow for imaging adjustments. All of the videos shown in the figures and supplemental materials were captured using a single specimen. The electron transparent region was a sample comprised of both matrix and twin orientations (Figure 1b).

Advantages/Drawbacks of In-situ Mechanical Testing

The in-situ mechanical testing technique described here has been successfully implemented in the past to study twinning in hcp metals [3,4]. The technique itself presents several unique advantages. The most obvious is time resolution of microstructural features. By directly observing the material during deformation, it is possible to identify active deformation mechanisms. Additionally, in-situ straining makes it possible to segregate defects and other microstructural features actively contributing to the observed behavior from those that are

present but inactive. Such a determination can be made only indirectly with conventional post-mortem analyses.

Additionally, because the specimens are prepared using precise FIB milling, the cross-sectional area of the thin foil is approximately rectangular. This results in a stress state very close to pure uniaxial tension. This technique differs from other methods for in-situ mechanical testing of TEM foils, where a conventional foil is mounted in the center of a tensile dogbone. When straining a conventional TEM foil, the region of interest is near a hole, which acts as a stress concentrator, giving rise to stress states that can be challenging to predict and interpret. Also, the amount of thin area in a conventional foil is much greater than that of a FIB-prepared foil, making it much more difficult to ensure that a given region of interest will deform under load. The reduced area of a FIB-prepared specimen makes it certain that deformation will occur in the viewing area, and almost guarantee that these deformation events can be captured. Because the orientations of the region of interest is known in advance for the site-specific technique, it is easier to ensure that the sample will be oriented correctly with respect to the loading axis, as well. This simplifies the effective stress state, and produces higher success rates than those expected when straining conventional TEM specimens.

The technique is not without disadvantages. One such obstacle is that, with the straining TEM specimen holder employed here, an axis of tilt is sacrificed for loading capabilities. This tends to make imaging more difficult in general. Some features may not be visible with suitable contrast without the crystallographic freedom afforded by two independent tilt axes. This can be minimized through careful planning when the specimens are sectioned from bulk during FIB processing. Even so, detailed character of defects is sometimes impossible to determine from an in-situ specimen alone. In these cases, it is necessary to compare observed defects and structures to those seen in conventional TEM foils that can be analyzed using a conventional dual-tilt TEM holder, and therefore characterized completely. Such comparisons between in-situ and post-mortem samples are possible because of the orientation information known in advance from EBSD. Detailed knowledge of initial orientations of both the matrix and twins greatly streamlines interpretation of observed microstructural features. A detailed understanding of the microstructure allows for the in-situ specimens to be benchmarked against, and compared to, post-mortem samples prepared by traditional means and characterized using a conventional TEM holder. Additionally, because the specimens are prepared using FIB, some amount of ion damage is expected, often manifested as a speckle pattern of dark spots. The amount of damage is heavily dependent on the material being studied. The damage layer is confined to the material ~1-3 nm at the surface, and is not expected to heavily influence the behavior of defects in the center of the foil. There is also no evidence that twin interface movement is affected.

The specialized holder use in the present work does not have the capability to measure stress and strain in real-time. Displacement can be determined directly through the holder instrumentation, or through observation of fiducial marks in the microstructure. Because the load is applied to a larger dogbone, the stress across the thin foil section is unknown. Despite this, the technique is well suited to study individual microstructural features and events known to occur under typical conditions.

It is important to note that there may exist certain thin film effects due to the geometry of the specimen. Nevertheless, in-situ straining experiments are conducted to gain insight into the active deformation mechanisms and contribute to the understanding of bulk behavior. All in-situ findings were compared against the wealth of post-mortem information in the literature, for consistency in end-point structures after deformation.

Results and Discussion

The evolution of microstructure in hcp metals involves both dislocations and twinning. Post-mortem examinations have been employed in the past to study both mechanisms. The behavior during deformation, and the interaction between mechanisms is extremely difficult to interpret using post-mortem techniques alone, making the in-situ straining technique especially attractive. Several unique scenarios are studied here to elucidate mechanical response during plasticity in magnesium.

Twin Boundary Movement

Given the prevalence of twins in magnesium following deformation, the motion of twin boundaries is incredibly important to the deformation behavior. Several hypotheses for twin boundary motion have been proposed which involve either the nucleation and motion of twin dislocations or atomic shuffle mechanisms [36–43]. In-situ straining brings a unique perspective to the motion of twin boundaries, as they can be observed directly. Previous work observed twin boundaries interacting with other twins [4,34], so the current study will focus on twin interactions with dislocations.

A tensile force was applied to a specimen containing a twin boundary oriented favorably for growth (motion into the parent), and the resulting boundary movement was observed. Figure 3 shows key frames from an in-situ loading video (available as supplemental material). The resolution of the video is insufficient to capture individual twinning dislocations moving along the boundary, however, several key observations can be made. Primarily, as the twin boundary grows, the interface between twin and matrix sweeps through dislocations that were present in the matrix. Through previous post-mortem examinations and current observations, dislocations in the parent matrix are known to lie on basal planes, while dislocations within the twinned regions can be either <a>-type basal dislocations or <c+a> dislocations lying in other planes [4]. It is reasonable to expect that the interaction between previously existing dislocations in the matrix and an encroaching twin boundary will modify the character of the dislocation as the boundary moves through. Such a mechanism has been proposed by Basinski *et al*. [44]. The reaction between a dislocation and a twin boundary should produce dislocation content within the twin, and these dislocations should be sessile. A post-mortem study of Zr by Bhattacharyya *et al.* [45] observed dislocations within twins, believed to be remnants of a twin-dislocation interaction. However, some of the dislocations were believed to be mobile. Determining the origin, character, and mobility of dislocations within twins is of utmost importance to models for work hardening of hcp materials. Figure 3 shows an ideal case to study this behavior. Both twin (lower left) and matrix (upper right) share a common zone axis, parallel to the viewing direction. Twin growth (for this $\{10\bar{1}2\}$ twin) can be characterized by an 86° rotation about the viewing axis. Due to limited contrast conditions and steeply inclined line direction relative to the viewing direction, dislocations within the matrix are difficult to resolve (but were observed), in Figure 3, but are consistent with basal dislocations seen in post-mortem analysis [4]. Such dislocations

have a line direction nearly perpendicular to the plane of the image, and appear as a dark point in the images shown. Because of their inconspicuous appearance, they are most apparent when they move, as seen in the supplemental video. Dislocations in the twin have much different character. Dislocation line segments were observed to be created in the twin (at the twin boundary) as the boundary moved through the microstructure. Interestingly, in at least one case (i.e. the green dislocation shown in Figure 3) the dislocation was tied to a specific location on the twin boundary and subsequent dislocation content was created at or very near that spot, which moved with the boundary (parallel to the motion of the twin boundary, not laterally along the boundary). Similar behavior is shown by the red dislocation in Figure 3, but the dislocation adopts a slightly different line direction. Each dislocation is at least partially mobile as new content is created during boundary movement (see supplemental video). The video of in-situ straining leads to the conclusion that the newly created dislocation content contains both sessile and glissile segments. Additionally, dislocation content lies on both basal and pyramidal planes. The experimentally observed behavior differs from that expected from a purely geometric transformation of dislocations as the twin boundary passes through, as in [46]. This is not to say that geometric transformations do not play a part in the final dislocation configurations, only that it cannot represent the entire mechanism. Figures 4 and 5 show two schematics for dislocation behavior as the twin boundary moves through. Figure 4 shows the case for parent matrix dislocations being converted by a twin boundary. The black line represents an array of basal dislocations in the parent similar to those observed experimentally. The segment in green shows the likely location of newly created dislocation content. Most notably, the point of contact between the converted segment inside the twin and the unconverted dislocation in the matrix should follow the dislocation in the matrix. This would have the effect of moving the inflection point laterally along the boundary as the twin moves through. In contrast, Figure 5 shows a schematic of the observed behavior, where dislocation line length is created in the twin by a mobile twin boundary. The green segment again shows the new dislocation formed inside the twin. In this case, the dislocation content in the matrix would be consumed at the twin boundary and new content is created behind. This latter scenario seems to more closely match the experimentally observed dislocation behavior in Figure 3. The observed dislocation behavior, coupled with the fact that newly created dislocation content adopts multiple planes for a single dislocation, disproves the Basinski mechanism of dislocation transformation associated with twin passage, which would predict the formation of a sessile dislocation in the same position as the glissile had in the matrix. In reality, a complex dislocation reaction is likely to take place at the twin boundary, with the creation of twin boundary (TB) dislocations being subsequently dragged by the boundary, plus glissile or sessile dislocations segments being incorporated in the twin domain [47].

Interaction of dislocations with second-generation twin

In previous work [3], the specimen shown in Figure 3 was studied with regard to detwinning under compressive load. In that study, a second-generation twin nucleated and grew inside the first-generation twin. The development of new dislocation content within the primary twin poses a unique opportunity, as the origin of these dislocations is known to be a result of twin growth. The second-generation twin is then interacting with complex character dislocations, which should result in even more complex dislocation structures. This was originally thought to hinder

dislocation motion, and it was hypothesized that this would lead to an eventual hardening effect as more dislocations become sessile.

Figure 6 shows dislocations that have interacted with the second-generation twin. A single dislocation of interest is highlighted in red to show its shape as the material is deformed in tension, shrinking (detwinning) the second-generation twin. Several sharp changes in line direction are observed along the dislocation line length. It is tempting to assume that this discontinuity in line direction demarcates the dislocation length that has been interacted with the twin boundary, and this would be the likely conclusion from post-mortem analysis. However, examination of the images in Figure 6 show that the dislocation length is mobile, moving and adjusting shape as the material is strained. This behavior is unexpected based on the mechanism proposed by Basinski, as the transformed dislocations should be sessile, and the transformed line length from a single dislocation is predicted to be a single line direction rather than multiple distinct line directions as observed. The enduring mobility of the dislocation lengths, even after interaction with multiple twin boundaries implies a few things. First, despite the complex character of the dislocations with twins, the dislocations are able to retain mobility, possibly through immediate dissociation into mobile segments. It is important to note that these dislocation segments closely resemble dislocations observed within twins during post-mortem examinations [4]. Also, this unexpected mobility of dislocations probably contributes to continued bulk plasticity during deformation, increasing overall ductility, and should be included in models of material hardening.

Conclusions

In-situ mechanical testing can yield complementary information to traditional post-mortem analysis. It is especially well-suited to collect data that has time resolution, which is critical to determine which deformation mechanisms are active, and the kinetics of such mechanisms. As novel examples of this, the creation of dislocation content within a twin was demonstrated, as well as the continued mobility of dislocations that had interacted with a twin boundary. Dislocation morphology in the twinned region suggests that dislocation content is created behind the moving twin boundary rather than by transformation of existing dislocations in the matrix. Determinations of mobility would be difficult using post-mortem techniques alone, and some microstructural features, notably sharp changes in line direction along dislocations near twin boundaries, are potentially misleading without considering the dislocation behavior during straining. Dislocations that had interacted with a twin boundary were shown to maintain mobility. In-situ straining has contributed significantly to several cases where a complete picture of material behavior is inaccessible or unclear using previously deformed, static samples. As such, there continues to be an opportunity to apply such experimental techniques to unique materials challenges, including exploration of strength and damage mechanisms, interactions between mechanisms, and time-dependent processes like creep and material aging.

Acknowledgements

This work was fully funded by the Department of Energy, Basic Energy
Science Project FWP06SCPE401. LA-UR-15-21099.

Supplemental Material

Full videos from which the screenshots from Figures 3 and 6 were taken are available as

supplemental material. Frames have been aligned to fiducial features to eliminate specimen shift due to straining.

References

1. Q. Yu, J. Zhang, and Y. Jiang, *Philos. Mag. Lett.* 91, 757-765 (2011).

2. C. J. Boehlert, Z. Chen, I. Gutiérrez-Urrutia, J. Llorca, and M. T. Pérez-Prado, *Acta Mater.* 60, 1889-1904 (2012).

3. B. M. Morrow, R. J. McCabe, E. K. Cerreta, and C. N. Tomé, *Metall. Mater. Trans. A* 45, 36-40 (2014).

4. B. M. Morrow, E. K. Cerreta, R. J. McCabe, and C. N. Tomé, *Mater. Sci. Eng. A* 613, 365-371 (2014).

5. C. C. Aydiner, J. V Bernier, B. Clausen, U. Lienert, C. N. Tomé, and D. W. Brown, *Phys. Rev. B* 80, 24113-1-6 (2009).

6. T. R. Bieler, L. Wang, A. J. Beaudoin, P. Kenesei, and U. Lienert, *Metall. Mater. Trans. A* 45, 109-122 (2014).

7. D. W. Brown, A. Jain, S. R. Agnew, and B. Clausen, *Mater. Sci. Forum* 539-543, 3407-3413 (2007).

8. D. W. Brown, S. R. Agnew, M. A. M. Bourke, T. M. Holden, S. C. Vogel, and C. N. Tomé, *Mater. Sci. Eng. A* 399, 1-12 (2005).

9. E. P. Butler, *Reports Prog. Phys.* 42, 833-889 (1979).

10. T. Imura and H. Fujita, *J. Electron Microsc.* 28, 33-36 (1979).

11. A. Couret, J. Crestou, S. Farenc, G. Molenat, N. Clement, A. Coujou, and D. Caillard, *Microsc. Microanal. Microstruct.* 4, 153-170 (1993).

12. P. B. Hirsch, R. W. Horne, and M. J. Whelan, *Philos. Mag.* 1, 677-684 (1956).

13. M. J. Whelan, P. B. Hirsch, R. W. Horne, and W. Bollmann, *Proc. R. Soc. Lond. A. Math. Phys. Sci.* 240, 524-538 (1957).

14. J. E. Bailey, *J. Nucl. Mater.* 7, 300-310 (1962).

15. H. G. F. Wilsdorf, *Rev. Sci. Instrum.* 29, 323-324 (1958).

16. H. Fujita, *J. Phys. Soc. Japan* 26, 331-338 (1969).

17. E. Furubayashi, *J. Phys. Soc. Japan* 27, 130-146 (1969).

18. I. Baker, E. M. Schulson, and J. A. Horton, *Acta Metall.* 35, 1533-1541 (1987).

19. D. Caillard, *Acta Mater.* 58, 3493-3503 (2010).

20. W. A. T. Clark, C. E. Wise, Z. Shen, and R. H. Wagoner, *Ultramicroscopy* 30, 76-89 (1989).

21. A. Couret and D. Caillard, *Acta Metall.* 33, 1447-1454 (1985).

22. S. Farenc, D. Caillard, and A. Couret, *Acta Metall. Mater.* 41, 2701-2709 (1993).

23. S. Ikeno, *Phys. Status Solidi A* 12, 611-622 (1972).

24. K. Konopka, J. Mizera, and J. W. Wyrzykowski, *J. Mater. Process. Technol.* 99, 255-259 (2000).

25. F. Louchet, L. P. Kubin, and D. Vesely, *Philos. Mag. A* 39, 433-454 (1979).

26. T. Tabata, H. Mori, H. Fujita, and I. Ishikawa, *J. Phys. Soc. Japan* 40, 1103-1111 (1976).

27. S. Zghal, A. Menand, and A. Couret, *Acta Mater.* 46, 5899-5905 (1998).

28. P. G. Partridge, *Metall. Rev.* 12, 169-194 (1967).

29. B. M. Morrow, S. N. Mathaudhu, E. K. Cerreta, J. P. Escobedo-Diaz, and D. R. Trinkle, *Metall. Mater. Trans. A* 45, 5876 (2014).

30. B. M. Morrow, R. W. Kozar, K. R. Anderson, and M. J. Mills, *Acta Mater.* 61, 4452-4460 (2013).

31. G. Proust, C. N. Tomé, and G. C. Kaschner, *Acta Mater.* 55, 2137-2148 (2007).

32. R. J. McCabe, G. Proust, E. K. Cerreta, and A. Misra, *Int. J. Plast.* 25, 454-472 (2009).

33. B. M. Morrow, R. J. McCabe, E. K. Cerreta, and C. N. Tomé, *Mater. Sci. Eng. A* 574, 157-162 (2013).

34. B. M. Morrow, R. J. McCabe, E. K. Cerreta, and C. N. Tomé, *Metall. Mater. Trans. A* 45, 5891-5897 (2014).

35. R. D. Field and P. A. Papin, *Ultramicroscopy* 102, 23-26 (2004).

36. J. W. Christian and S. Mahajan, *Prog. Mater. Sci.* 39, 1-157 (1995).

37. L. Capolungo, I. J. Beyerlein, and C. N. Tomé, *Scr. Mater.* 60, 32-35 (2009).

38. R. C. Pond and S. Celotto, *Metall. Mater. Trans. A* 33, 801-807 (2002).

39. A. Serra and D. J. Bacon, *Philos. Mag. A* 73, 333-343 (1996).

40. S. G. Song and G. T. Gray III, *Acta Metall. Mater.* 43, 2325-2337 (1995).

41. H. Wang, P. D. Wu, J. Wang, and C. N. Tomé, *Int. J. Plast.* 49, 36-52 (2013).

42. J. Wang, L. Lei, C. N. Tomé, S. X. Mao, and S. K. Gong, *Mater. Res. Lett.* 1, 81-88 (2013).

43. J. Wang, S. K. Yadav, J. P. Hirth, C. N. Tomé, and I. J. Beyerlein, *Mater. Res. Lett.* 1, 126-132 (2013).

44. Z. S. Basinski, M. S. Szczerba, M. Niewczas, J. D. Embury, and S. J. Basinski, *Rev. Metall.* 94, 1037-1043 (1997).

45. D. Bhattacharyya, E. K. Cerreta, R. McCabe, M. Niewczas, G. T. Gray III, A. Misra, and C. N. Tomé, *Acta Mater.* 57, 305-315 (2009).

46. M. Niewczas, *Acta Mater.* 58, 5845-5857 (2010).

47. J. Wang, I. J. Beyerlein, and C. N. Tomé, *Int. J. Plast.* 56, 156-172 (2014).

Figures

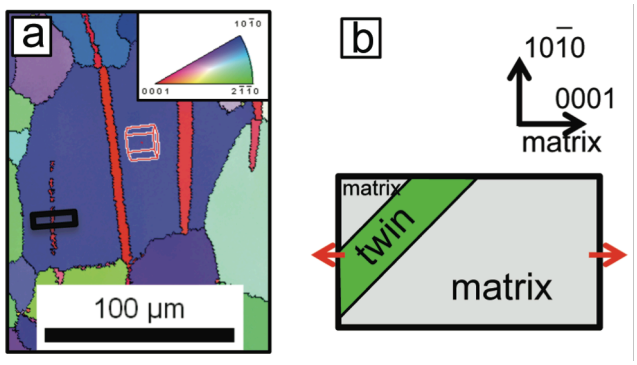

Figure 1. (a) EBSD scan of the region of interest from which a small foil was prepared, and **(b)** schematic of resulting TEM foil, which represents a 90 degree rotation from the orientation shown in (a). The matrix is oriented with the c-axis parallel to the tensile axis (red arrows in (b)), promoting twin growth.

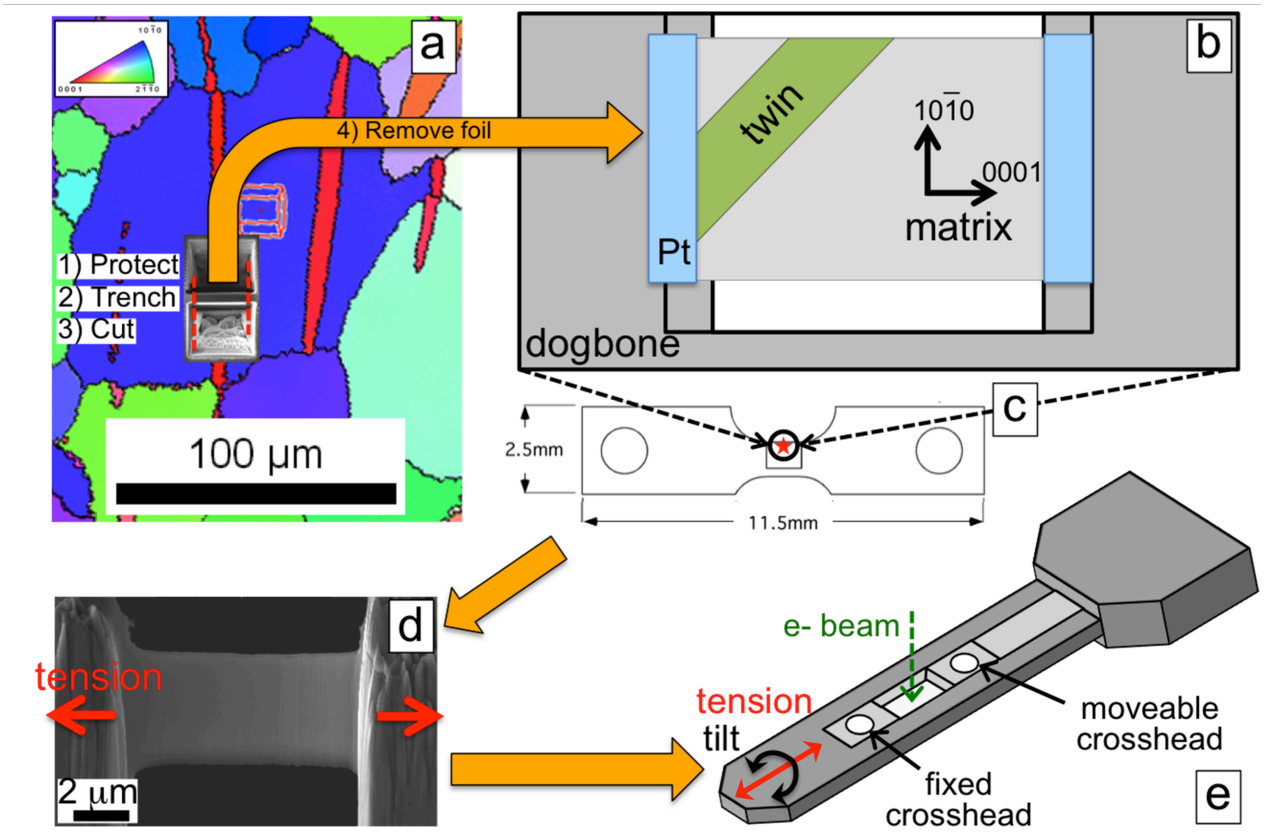

Figure 2. In-situ mechnical test preparation technique. a) Samples are prepared, extracted, manipulated, and tacked to a larger dogbone specimen using common FIB techniques. b) Schematic of the center section of the tensile dogbone to which the TEM foil is secured. c) Schematic of the complete tensile dogbone. d) SEM image of the thinned foil, mounted in the center of the tensile dogbone before straining. e) Schematic of a commercially available TEM holder used to exert force on the sample.

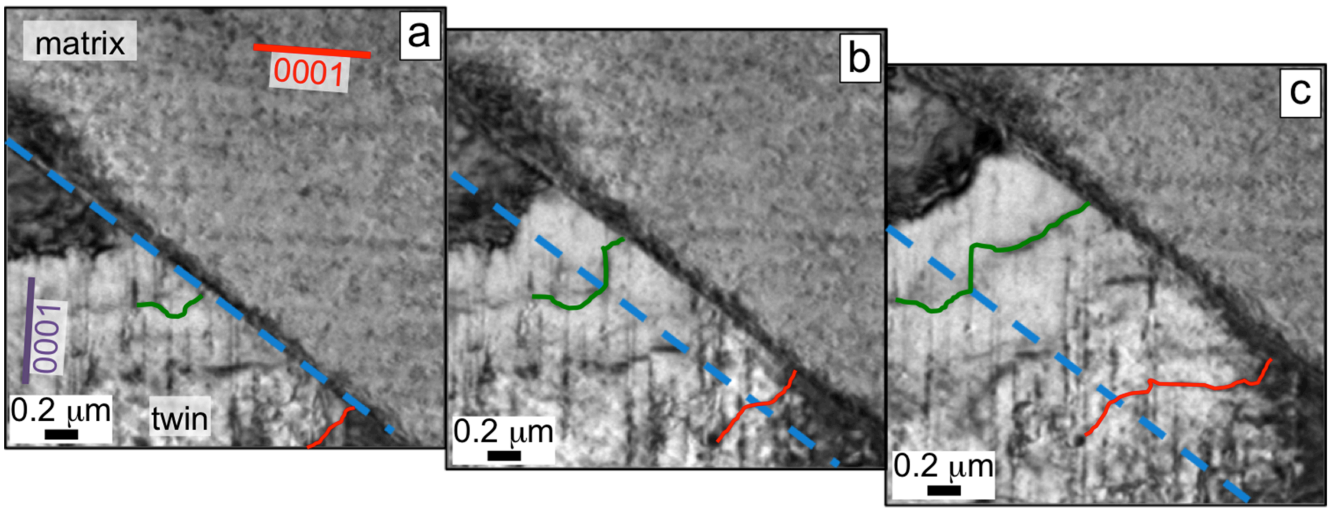

Figure 3. Selected frames from video of in-situ straining. A twin boundary moves towards the top right corner of the frame under tensile load. The time (t) for each frame corresponds to: a) t = 0 s, b) t = 24 s, and c) t = 48 s. The dashed blue line denotes the original location of the boundary.

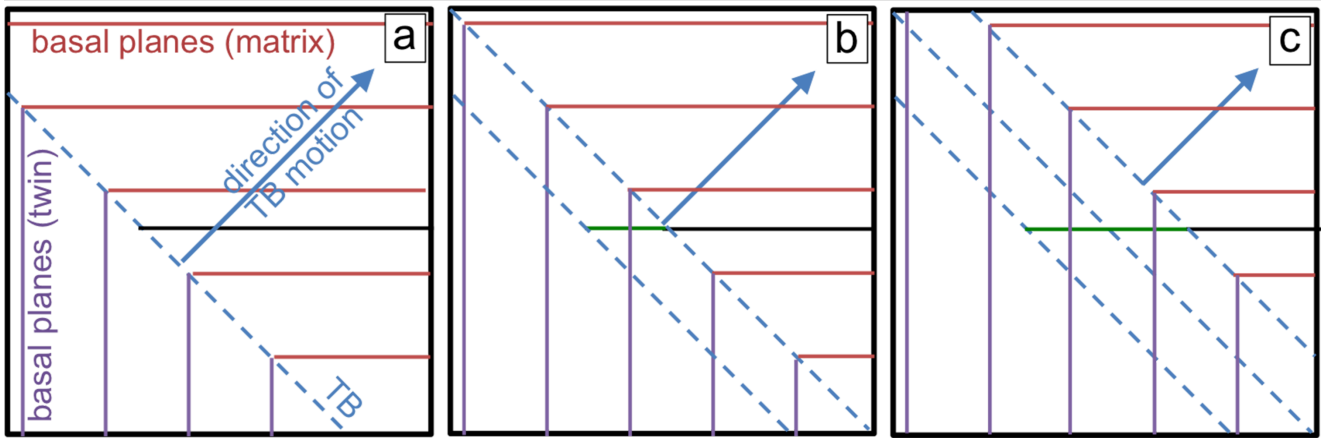

Figure 4. Schematic of the theoretical appearance of dislocations assuming a rotation of the lattice due to twinning. The dislocation content prior to and following interaction with a twin boundary is shown in black and green, respectively. Three different time steps are shown in a-c, which roughly correspond to Figure 3 a-c, respectively.

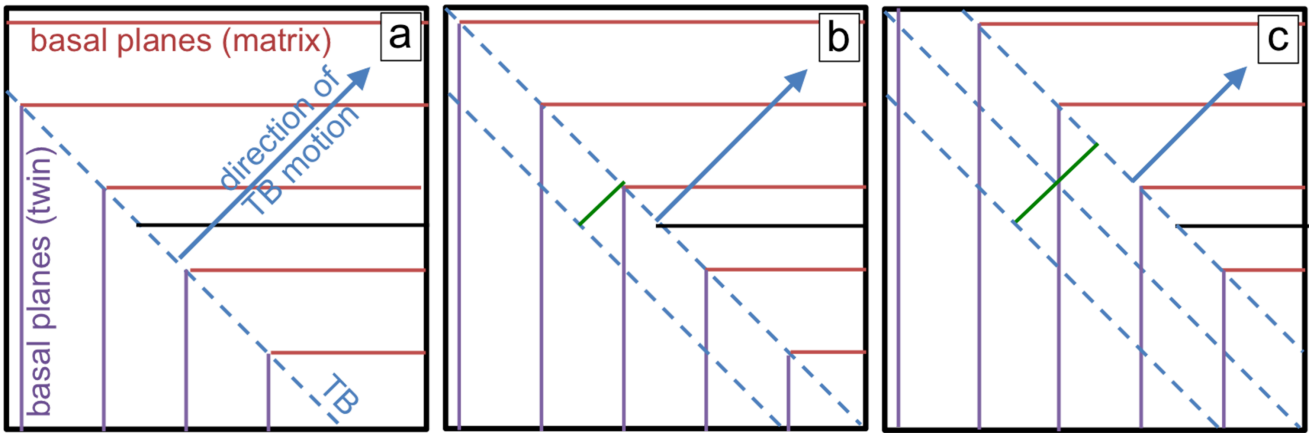

Figure 5. Schematic of the theoretical appearance of dislocations assuming new content is created behind the twin front. This type of mechanism leads to a discontinuity at the twin boundary. Three different time steps are shown in a-c, which roughly correspond to Figure 3 a-c, respectively.

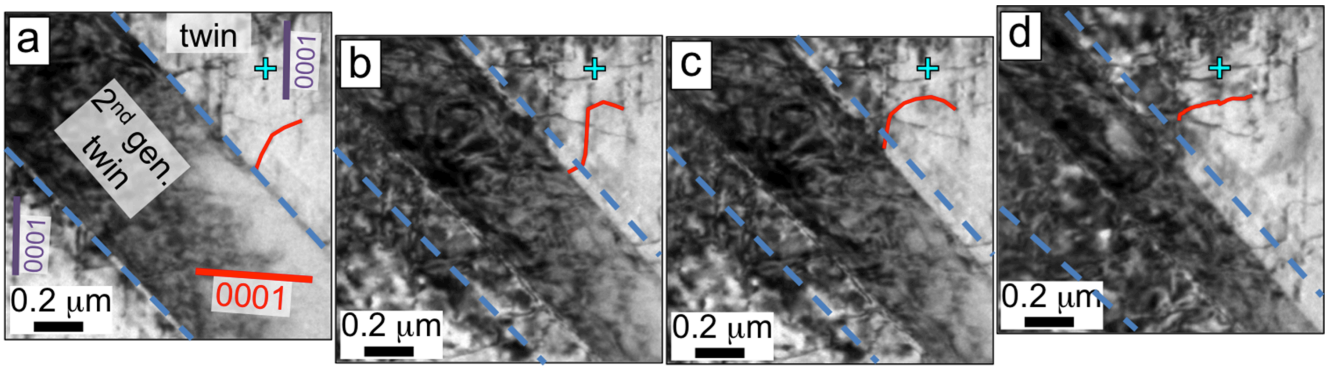

Figure 6. Frames from video showing dislocation motion after multiple interactions with twin boundary. The time (t) for each frame corresponds to: a) t = 0 s, b) t = 5.4 s, c) t = 6.1 s, and d) t = 7.1 s. The dislocation is highlighted in red, while a blue cross represents a fiducial mark for comparison between frames. The blue dashed line represents the original location of the second-generation twin.